Journal of Applied Geophysics 171 (2019) 103866

Contents lists available at ScienceDirect

Journal of Applied Geophysics

journal homepage: www.elsevier.com/locate/jappgeo

Bedrock depth evaluation using microtremor measurement: empirical guidelines at weathered granite formation in Singapore

Sung-Woo Moon [a,1], Palanidoss Subramaniam [b], Yunhuo Zhang [b], Ganapathiraman Vinoth [c], Taeseo Ku [b,*]

[a] Department of Civil and Environmental Engineering, Nazarbayev University, 53 Kabanbay Batyr Ave, Nur-Sultan 010000, Kazakhstan
[b] Department of Civil and Environmental Engineering, National University of Singapore, 1 Engineering Drive 2, Singapore 117576
[c] Department of Civil Engineering, The University of British Columbia, 6250 Applied Science Lane, Vancouver, BC V6T 1Z4, Canada

ARTICLE INFO

Article history:
Received 30 May 2019
Received in revised form 30 August 2019
Accepted 3 October 2019
Available online 15 October 2019

Keywords:
Microtremor array measurement
Microtremor measurement
Phase velocity
Shear wave velocity
Bedrock detection
Horizontal to vertical spectral ratio

ABSTRACT

Detection of bedrock depth is one of the critical site investigation procedures for seismic hazard analysis and underground developments that may encounter varying rock formation. The most common practice to detect bedrock is to directly drill boreholes. However, the intrusive borehole-based site investigation process is often expensive and time consuming and provide limited information from discrete boreholes. In the present study, a surface wave based technique, microtremor array measurement (MAM) and microtremor measurement (MM) is used to find the depth of bedrock at Bukit Timah granite formation in Singapore. Based on a series of MAM and/or MM surveys, four interpretation approaches, i.e., (1) Bilinear intersection method; (2) Preselected shear wave velocity (V_S) based approach; (3) Normalized phase velocity approach; and (4) Horizontal to vertical spectral ratio (HVSR) analysis, are proposed for bedrock depth detection. The first three approaches are based on surface wave inverted V_S profile using a vertical component of MAM. The fourth approach is to utilize the natural frequency of the ground through HVSR using three components microtremor measurements (MM). By compiling experimental data at nine different testing sites, it was demonstrated that non-invasive surface wave-based approaches can be effectively used for bedrock detection. Especially, a promising empirical correlation between the natural frequency of ground and the depth of bedrock is subsequently proposed.

1. Introduction

In underground development, uncertainty due to unforeseen ground condition may cause delays and incidents in construction. A variety of technical challenges which might occur during underground construction should be predefined by a comprehensive site investigation program. Detection of bedrock depth is critical and can provide essential information for various objectives in geotechnical developments: (a) foundation design including appropriate types (e.g., shallow or deep) and location; (b) information on selecting appropriate equipment for excavation or drilling; (c) ideal location of underground tunnels. In addition, it has a significant influence on not only seismic site classification using average shear wave velocity of top 30-m soil layers (Anbazhagan et al., 2012), but also site amplification on seismic hazard assessment (Koesuma et al., 2017).

To assess the subsurface strata and to locate the particular depth of rock, most of the site investigation practices typically follow conventional borehole programs which involve traditional drilling, sampling, and laboratory testing as well as specific in-situ testing. Thus, in terms of conventional site investigations, detailed and accurate underground survey requires intensive boreholes which are rather time consuming and costly. Compared to the conventional site investigations, various geophysical methods such as seismic, gravity, electromagnetic, and magnetic surveys are considered to be possible alternatives which may be relatively fast, economical, less/non-intrusive and efficient. For example, Beauvais et al. (1999) attempted to characterize the geometry of the soil layers above high-resistivity granitic bedrock using electrical resistivity tomography (ERT). Also, Zhou et al. (2000) measured irregular bedrocks in karst terranes via ERT, taking advantage of high contrast of resistivity between the clayey soil and limestone. Nevertheless, it is important to aware that ERT is sensitive to variations in electrical conductivity of subsurface materials, though rock is generally less conductive than soil or sediment, not the rocks of clay-rich or water filled that may be more conductive than some soils (e.g. dry

* Corresponding author.
E-mail addresses: sung.moon@nu.edu.kz (S.-W. Moon), psmani100@gmail.com (P. Subramaniam), zhangyunhuo@u.nus.edu (Y. Zhang), gv1134@mail.ubc.ca (G. Vinoth), ceekt@nus.edu.sg (T. Ku).
[1] (former Post-doctoral Research Fellow, National University of Singapore).

https://doi.org/10.1016/j.jappgeo.2019.103866

gravel, sand/silt). The efficiency of ERT was decreased when the bedrock exhibited poor resistivity contrasts with the upper soil layers (Coulouma et al., 2010).

With the enhancement in seismographs and processing software, it is suitable to apply the seismic refraction method for shallow subsurface exploration (<30 m) without any explosive source (Martínez and Mendoza, 2011; Sloan et al., 2013). For investigation of greater depths (>30 m), seismic reflection involving analysis of the entire wave of seismic energy arriving at an array of geophones from a shot point may be preferred (Malinowski, 2016). However, the technique may be not applicable in the regions with considerable layer alterations (e.g., effect of significant reflection/refraction noises). Where borehole seismic technologies are available, hole-to-hole or hole-to-surface seismic tomography data can also be collected (using downhole geophones and a source) to improve the resolution of either the seismic refraction or reflection surveys. However, generally the invasive borehole geophysics are rather expensive and provide only limited testing information at the selected location.

For surface wave, Aki (1957) explicitly computed spatial autocorrelation coefficients among the Rayleigh waves recorded at different locations. Subsequently, dispersion characteristics of Rayleigh waves and inversion techniques were explored to generate the shear wave velocity (V_S) profile (Nazarian and Stokoe, 1984; Tokimatsu et al., 1992; Xia et al., 1999). Especially, a passive-source surface wave technique is an eco-friendly (less environment impact) method for geotechnical survey. For example, using the surface wave measured by microtremor array measurement (MAM) and processed by spatial autocorrelation (SPAC), Okada and Suto (2003) explored the subsurface (100 m to kilometers) and Hayashi (2008) similarly applied it to shallow site investigations (10 m–100 m) to generate a V_S profile. Recently, the combined active MASW and MAM was employed to estimate the bedrock depth, based on a preselected wave velocity of rock and/or the normalized Rayleigh wave dispersion curve at a specific site in Singapore (Moon et al., 2017; Moon et al., 2016; Moon and Ku, 2017).

In this study, we propose more effective methodologies utilizing only passive-source surface waves based on the conventional MAM and microtremor measurements (MM) with a three-component (i.e., one vertical and two horizontal) geophone, which enables site-specific detection of bedrock depth. To build a comprehensive database, a series of MAM and MM were carried out at various site locations at Bukit Timah granite region, Singapore where the bedrock varies from 10 m–70 m with an average of around 30 m (Sharma et al., 1999; Zhao, 1998). Firstly, based on the MAM, three independent approaches are proposed to find the bedrock depth. Secondly, a new empirical correlation is established between the natural frequency of the ground calculated from the MM and the bedrock depth from conventional borehole drilling towards its application at Bukit Timah granite. Finally, the efficacy of the different approaches proposed to detect bedrock depth is assessed using conventional bore log information as reference.

2. Site information

Fig. 1 presents the geological materials of Singapore comprising four main types: (1) igneous rocks (Bukit Timah granite and Gombak norite); (2) sedimentary rocks (Jurong formation); (3) Quarternary deposit (Old Alluvium); and (4) recent alluvial deposit (Kallang formation) (Pitts, 1983; Sharma et al., 1999). Residual soils from two geological formations such as the Bukit Timah granite formation and the Jurong sediment formation cover approximately two-thirds of Singapore's land area (Rahardjoa et al., 2004; Winn et al., 2001). Bukit Timah granite distributed in the central part of Singapore is considered as base rock of Singapore as it is underlying other geological formations. Due to the humid climate, tropical rainfalls and the presence of dense biological system, the Bukit Timah granite formation usually varies from residual soil (Grade VI) at shallow depth to intact rock (Grade I), as described in Table 1. The microtremor array measurement (MAM) tests were conducted at nine different locations in Bukit Timah granite formation in Singapore, as shown in Fig. 1. The geomaterial types at the testing locations can be broadly classified into three categories such as backfill soil, residual soil and completely weathered granite, and moderately and slightly weathered granite rock. Based on the non-invasive MAM and microtremor measurements (MM), this study intends to explore the possibility to locate the surface of the moderately weathered rock (Grade III) since mechanical properties and behaviors start to alter significantly from the Grade III (Sharma et al., 1999).

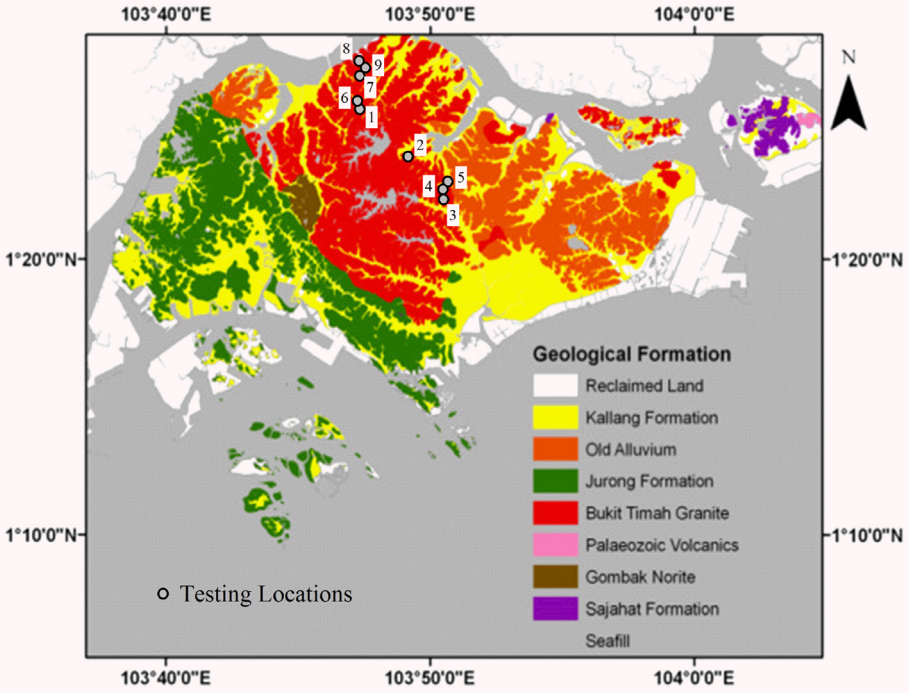

Fig. 1. Testing locations in the Bukit Timah granite formation (Modified from Lee and Zhou (2009)).

Table 1
Weathering classification for Bukit Timah granite and Gombak norite in Singapore (from British Standards Institution (1999)).

Grade	Basis for assessment
I	Intact strength, unaffected by weathering. Not broken easily by hammer rings when struck. No visible discolouration.
II	Not broken easily by hammer – rings when struck. Fresh rock colours generally retained but stained near joint surfaces.
III	Cannot be broken by hand. Easily broken by hammer. Makes a dull or slight ringing sound when struck with hammer. Stained throughout.
IV	Core can be broken by hand. Does not slake in water. Completely discoloured.
V	Original rock texture preserved, can be crumbled by hand. Slakes in water. Completely discoloured.
VI	Original rock structure completely degraded to a soil, with none of the original fabric remains. Can be crumbled by hand.

3. Experimental program

Generally, multi-channel analysis of surface wave (MASW) including active-source and passive-source (referred as microtremor array measurement (MAM)), and microtremor measurements (MM) have been employed for various geotechnical and geophysical applications (Foti et al., 2011; Lin et al., 2004; Moon et al., 2017; Moon and Ku, 2018; Moon et al., 2018; Rezaei and Choobbasti, 2017). In this study, MAM and MM surveys were conducted because the targeting bedrock depth in Bukit Timah granite formation is generally located in the range of 20–50 m.

Fig. 2 illustrates two types of data-acquisition systems of (a) MAM with one-component geophones and (b) MM with a three-component geophone. Basically, they employ ambient energy unintentionally generated from human activity and natural phenomena (Del Gaudio and Wasowski, 2011; Moon et al., 2017). In this study, MAM was conducted using 4.5-Hz vertical geophones with spike/tripod base connected to a 24 channel seismograph (Geode) developed by Geometrics (San Jose, California). In addition, a 4.5-Hz three-component geophone with 3-spike base was used for recording two horizontal components and a vertical component of microtremor simultaneously for the MM. Before taking the measurement, vertical geophones for MAM and three component geophones were securely aligned to the ground by a set of spikes/tripods.

A total of thirteen MAM tests with L-shape array and fourteen MM tests were performed at each borehole location, as indicated in

Table 2
A summary of testing programs conducted at Bukit Timah granite formation in this study.

Testing location	Borehole #	Testing methods	Array size	Geophone base (number of geophone)
Woodlands Ave 12	1.1	MAM (Passive-source)	50 m × 50 m	Spike (11)
		MM	–	Spike (3)
	1.2	MAM (Passive-source)	50 m × 50 m	Spike (11)
		MM	–	Spike (3)
Ang Mo Kio Park	2.1	MAM (Passive-source)	40 m × 40 m	Spike (11)
		MM	–	Spike (3)
	2.2	Active-source	34.5 m	Spike (24)
		MAM (Passive-source)	30 m × 30 m	Spike (11)
		MM	–	Spike (3)
Ang Mo Kio St 24	3.1	MAM (Passive-source)	40 m × 40 m	Tripod (11)
		MM	–	Spike (3)
	3.2	MAM (Passive-source)	40 m × 40 m	Tripod (11)
		MM	–	Spike (3)
Ang Mo Kio 3&6	4.1	Active-source	34.5 m	Spike (24)
		MM	–	Spike (3)
	4.2	MAM (Passive-source)	40 m × 40 m	Spike (11)
		MM	–	Spike (3)
Woodlands Ave 1	5.1	MAM (Passive-source)	50 m × 50 m	Spike (11)
		MM	–	Spike (3)
	5.2	MAM (Passive-source)	50 m × 50 m	Spike (11)
		MM	–	Spike (3)
Woodlands Dr. 19	6	MAM (Passive-source)	40 m × 40 m	Spike (11)
		MM	–	Spike (3)
Woodlands St 81	7	MAM (Passive-source)	30 m × 30 m	Spike (11)
		MM	–	Spike (3)
Woodlands St 12	8	MAM (Passive-source)	40 m × 40 m	Tripod (11)
		MM	–	Spike (3)
Springleaf Garden	9	MAM (Passive-source)	40 m × 40 m	Spike (11)
		MM	–	Spike (3)

Note: Spike – Natural ground; Tripod – Pavement, Concrete floor

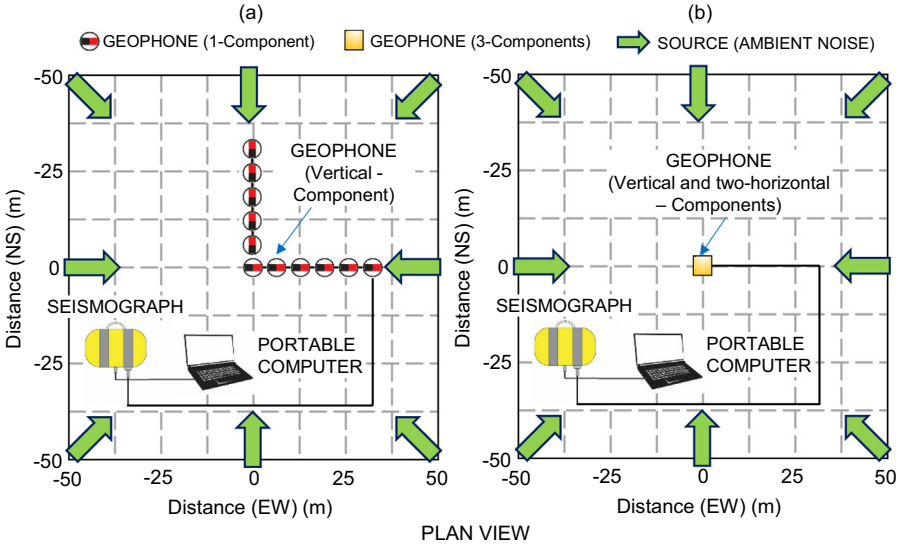

Fig. 2. Data acquisition system: (a) MAM with one-component geophones; (b) MM with a three-component geophone.

Table 2. Data acquisition during about 40-min intervals for MAM and 20-min intervals for MM were conducted using the Geometrics Geode. Additional active-source MASW tests were conducted at two borehole locations (i.e., 2.2 and 4.1) due to a smaller size of L-shape array (30 m × 30 m) at borehole #2.2 and very shallow bedrock depth at borehole #4.1. The reader is referred to Moon et al. (2017) for details of active-source MASW test and combined active and passive methods.

Fig. 3 illustrates the sequences of the typical MAM and MM data processing used in this study. Fig. 3(a) presents the waveform data on a vertical component recorded from MAM at 11 geophone locations, respectively. Thereafter, the phase velocity was determined using the SPAC method developed by Aki (1957) and Okada and Suto (2003), as shown in Fig. 3(b). The SPAC function in Eq. (1) is employed to find the average complex coherence function of the array and equate it with directional average of the trigonometric function which leads to the estimation of dispersion curve (Hayashi, 2008).

$$SPAC(x,\omega) = \frac{1}{2\pi}\int_{\varphi=0}^{\varphi=2\pi} Re(COH(x,\varphi,\omega))d\varphi = J_0\left[\left(\frac{\omega}{c(\omega)}\right)\times x\right] \quad (1)$$

where *COH* is complex coherence, x is the separation of two receivers, and φ is the direction of two receivers, J_0 is Bessel function, and $c(\omega)$ is phase velocity at angular frequency ω.

For the dispersion curve inversion, an initial model based on only the fundamental mode is constructed by one-third wavelength transformation in terms of apparent depth (D_A) and Rayleigh wave velocity (V_R) (Eqs. 2 and 3) (Moon et al., 2017).

$$D_A = a \times \lambda = a \times c/f \quad (2)$$

$$V_R = c = b \times V_s \quad (3)$$

where a is 1/3, λ is wavelength, c is phase velocity, f is frequency, and b is 0.9–0.95.

From the inversion process of phase velocity curve based on a non-linear least square method (LSM) (Xia et al., 1999), the corresponding shear wave velocity (V_S) model was generated (Fig. 3(c)). In order to obtain a stable and unique solution, the number of layers and thickness of each layer are fixed through the iteration process (Kumar et al., 2006).

Fig. 3(d) shows the ambient seismic noises on a vertical component and two horizontal components measured from MM. From the calculated Fourier spectrum for each trace (Fig. 3(e)), the horizontal to vertical spectral ratio (HVSR) was calculated (Fig. 3(f)) as follows:

$$\text{HVSR}(\omega) = \left[\left(S^2(\omega)_{NS} + S^2(\omega)_{EW}\right)/2S^2(\omega)_V\right]^{1/2} \quad (4)$$

where $S^2(\omega)_{NS}$ and $S^2(\omega)_{EW}$ are the horizontal spectra of north-south and east-west directions, respectively, and $S^2(\omega)_V$ is the vertical spectra. It was reported that different HVSR equations (equation itself) also do not have a significant effect on identifying a peak frequency and the adopted equation (Eq. (4)) can provide a reliable result in Singapore geology (Zhang and Ku, 2019). The following section explains the detailed methodology of each method proposed in this study.

4. Methodology for bedrock evaluation

From data acquisition and analysis of surface wave measurements, four independent approaches to estimate bedrock location are proposed using: 1) bilinear intersection; 2) preselected shear wave velocity (V_S); 3) normalized phase velocity (V_R); and 4) horizontal to vertical spectral ratio (HVSR). Fig. 4 illustrates a flow chart to estimate the depth of bedrock. The first three approaches are based on the conventional microtremor array measurement (MAM) processed by a spatial autocorrelation (SPAC) method, whereas the fourth approach is based on the three-component (i.e., one vertical and two horizontal) microtremor measurements (MM) processed by the horizontal to vertical spectral ratio (HVSR).

4.1. Bilinear intersection-based approach

This is an intuitive solution to estimate the depth of bedrock. The ground is simply assumed as a two-layer model which consists of soil and bedrock. The method infers the depth of bedrock based on a typical shape of V_S profile obtained from MAM. As noted, the top layer is considered as soil where the V_S increases with the increase in depth. The bottom layer is stiff strata where the moderately weathered rock (Grade III) presents. In this method, linear lines are drawn along the slope of the average V_S at each depth. It is assumed that the intersection point of the two straight lines corresponds to the depth of bedrock. For example,

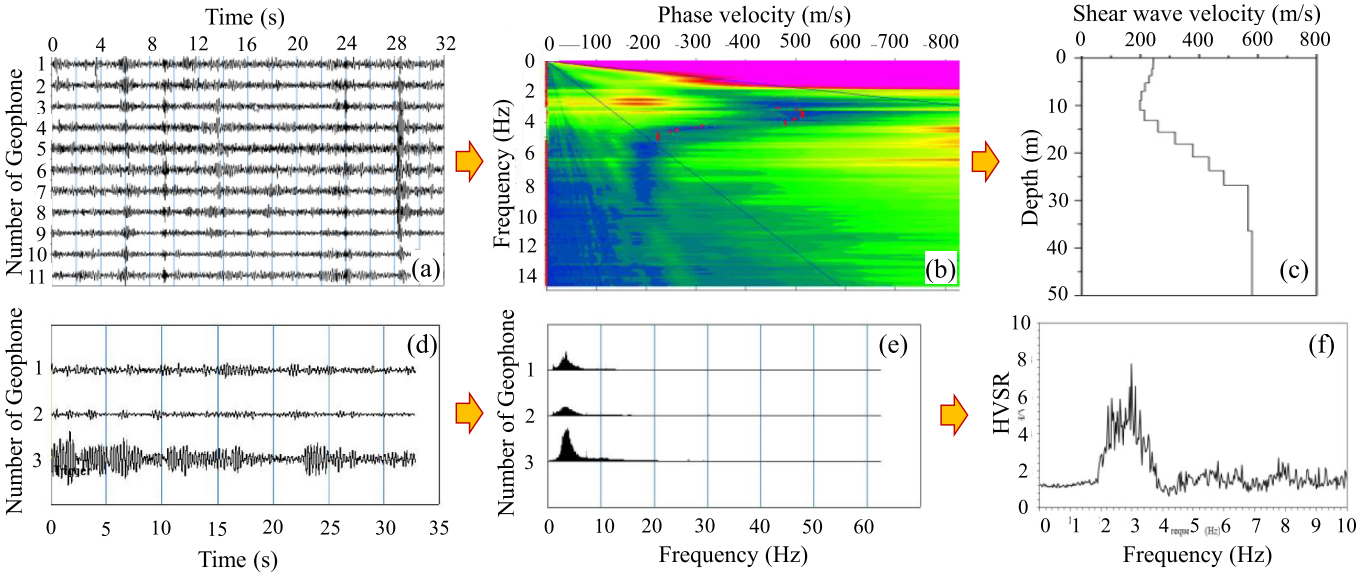

Fig. 3. Typical MAM and MM data processing sequences: (a) raw dataset obtained from MAM, (b) dispersion curve, (c) shear wave velocity profile, (d) waveform dataset from MM, (e) Fourier spectrum, and (f) HVSR.

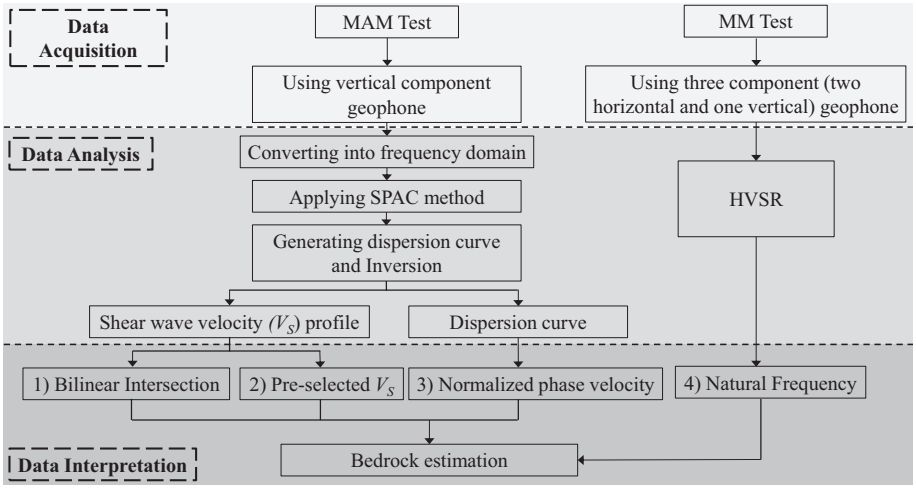

Fig. 4. Flow chart for the bedrock estimation in this study.

Fig. 5 shows a graphical example how to utilize the V_S profile for applying this approach at borehole #6. From 15 m to 30 m, V_S continuously increases with depth while beyond 30 m V_S increases with depth at a much slower rate. The two different rates of increase in V_S allow two straight lines to be drawn, one at a shallow depth (up to 30 m) and another for depth >30 m, approximately connecting the average V_S values at each depth. The intersection of the two straight lines indicates the depth of bed rock (i.e. 26.8 m). At borehole #6, the difference between bedrock locations estimated by the bilinear intersection-based approach and the reference borelog is found about 2.4 m (Fig. 5). It should be noted that the effect of confining pressure in rock is almost negligible on V_S, thus resulting in apparent distinction, as shown in Fig. 5. Bedrock depths at all test sites are estimated from the bilinear intersection-based approach, and the discussion of the results is followed in a subsequent section.

4.2. Preselected V_S-based approach

Pre-selecting the V_S value of bedrock surface would be the simplest approach to infer the depth of bedrock. In this approach, a reference V_S of bedrock is determined based on the generated V_S profile for each test site with the corresponding borehole information. From the MAM survey, it is found that the V_S values of bedrock surfaces in the Bukit Timah granite formation vary from 333 to 584 m/s. In order to facilitate the interpretation in a practicable manner, an average V_S value (456 m/s) on bedrock surfaces of all test sites was considered as preselected V_S ($V_{S(pre)}$) to estimate the depth of bedrock.

In order to apply the approach at Bukit Timah granite formation, a vertical line which has the $V_{S(pre)}$ of 456 m/s needs to be constructed together with the V_S profile obtained from MAM. If the vertical line encounters the V_S profile, then a horizontal line is drawn to find the corresponding bedrock depth. Moreover, two vertical lines corresponding to 392 m/s and/or 521 m/s ($V_{S(pre)} \pm$ standard deviation, SD) would be employed as alternative references. For example, Fig. 6 compares the two V_S profiles obtained from MAM at boreholes #1.2 and #3.2, respectively. As shown in Fig. 6, the V_S of borehole #3.2 is greater than that of borehole #1.2 in the range of 15–30 m, and it becomes smaller than that

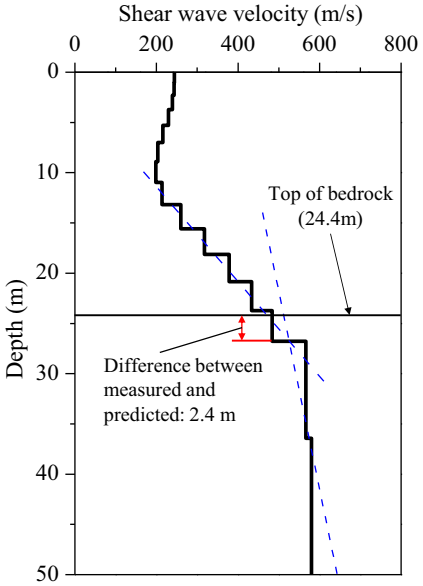

Fig. 5. Typical illustration of a bilinear intersection method at borehole #6.

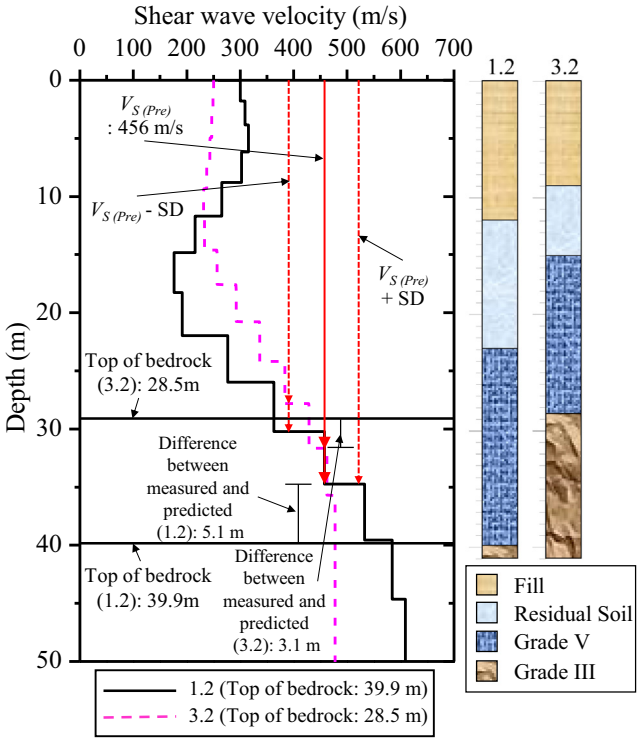

Fig. 6. Shear wave velocity profiles at two borehole locations (borehole #1.2 and #3.2).

of borehole #1.2 below a depth of 30 m. The $V_{S(pre)}$ of 456 m/s yields the estimated bedrock depth of 34.8 m and 31.6 m at borehole #1.2 and #3.2, respectively. The discrepancies between the bedrock depths predicted by the $V_{S(pre)}$ and observed from the reference borelog are about 5.1 m for borehole #1.2 and 3.1 m for borehole #3.2. In addition, the differences between the bedrock depths estimated by the $V_{S(pre)} \pm$ SD and borelog are in the range of 5.1–9.7 m for borehole #1.2 and 0.7 m ($V_{S(pre)}$ + SD: not applicable) for borehole #3.2. It is found that these pre-selected reference values work reasonably well as a rough estimation. The preselected V_S-based approach is applied to estimate bedrock depths at all test sites. The results will be further discussed in section 5.

4.3. Normalized Rayleigh wave phase velocity (V_R)-based approach

In previous studies, normalized Rayleigh wave phase velocity (V_R) was employed to estimate the depth to shallow bedrock (<10 m) from simulated master dispersion curves (Tamrakar and Luke, 2013) and the depth to bedrock between 28 and 36 m from combined active-source and passive-source MASW tests (Moon et al., 2017). It was inferred that bedrock depths could be estimated by normalizing the velocities of the dispersion curves due to impedance contrast between soil layer and rock formation.

In this study, dispersion curves observed from only MAM for each borehole location are normalized with respect to the V_R of the top layer on the dispersion curve and plotted against corresponding wavelength (λ). For example, Fig. 7 shows the dispersion curves normalized by V_R of 245 m/s and 252 m/s on the top layer at two borehole locations (2.1 and 3.2), respectively. From the bore logs (Borehole #2.1 and #3.2) details of testing site, the depths of bedrock (Grade III) are known as 39.9 m and 28.5 m. It is assumed that the depth of bedrock corresponds to 1/3 of wavelength (Moon et al., 2017). Thus, the wavelengths (λ) of 119.7 m and 85.5 m corresponding to each bedrock depth are calculated from where a vertical line is drawn to the normalized phase velocity curve. Subsequently, a horizontal line is drawn from the intersection point to find the normalized V_R. It is found that the normalized V_R are approximately 1.7 and 1.5 at the two borehole locations (1.2 and 3.2). The normalized V_R for all test sites are respectively determined for estimating bedrock depths.

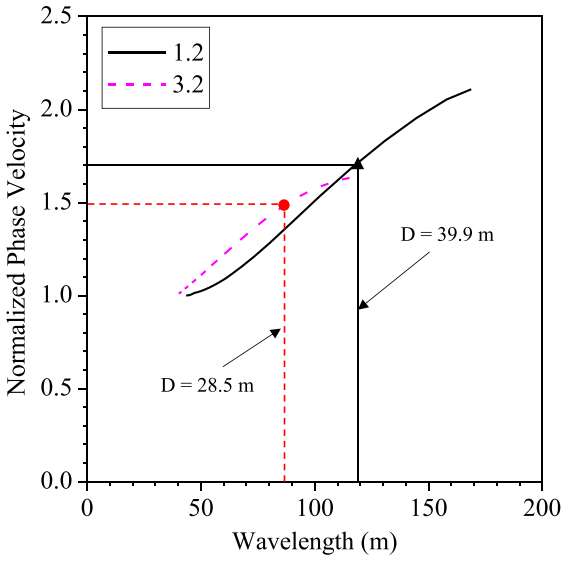

Fig. 7. Dispersion curves normalized by the top layer at two borehole locations (#1.2 and #3.2).

4.4. HVSR-based approach

In several previous studies, seismic noise measurements have been used for mapping the thickness of soft sediments (Delgado et al., 2000a; Delgado et al., 2000b; Ibs-von Seht and Wohlenberg, 1999). Nakamura (1989) described that the HVSR usually shows a peak point that depends on the subsoil profile. The observed peak corresponds to the site-specific natural frequency of the ground. In addition, the fundamental nature frequency is related to sediment's thickness which is the bedrock depth (Akkaya and Özvan, 2019; García-Jerez et al., 2007; Parolai et al., 2002; Rosenblad and Goetz, 2010). They showed that this method could be a promising method in the field where the impedance contrast is significant (e.g., stiff layer that has at least two times large impedance compared to sediment layer). However, most of previous studies are in the view of earthquake seismology where the interested rock depth is located at 100 m to kilometers.

In this study, HVSR is applied for identifying the top surface of Grade III weathered rock located above 50 m depth. The highly weathered rock (Grade IV) and residual soil (Grade VI) are considered as overburden. From the three-component seismic data captured, calculated Fourier spectra corresponding to horizontal components (EW & NS) are averaged and then divided by Fourier spectra of vertical component to find the spectral ratio. Then, HVSR is calculated in the frequency domain to find the fundamental resonance / natural frequency of the particular site. For instance, Fig. 8 shows the HVSR calculated for two of the analyzed sites. It indicates that the clear peaks in the HVSR are determined at each natural frequency (i.e., 2.53 Hz for borehole #1.2, and 2.87 Hz for borehole #3.2). Using the HVSR method, the natural frequencies at each test location are investigated for further analysis. The results are discussed in the following section.

5. Results and discussion

As mentioned at section 4.1 and 4.2, after deriving the V_S profiles, bedrock depths are estimated from the bilinear intersection-based approach, and the preselected V_S-based approach for the entire Bukit Timah granite formation region, as indicated in Table 3.

In order to identify the possibility of estimating the bedrock depths using the normalized V_R-based approach, the normalized phase velocities (V_R) corresponding to the observed bedrock depths (based on 1/3 wavelength) are selected and compiled from all the testing sites, as shown in Fig. 9. It is found that the normalized phase velocities fall in the narrow band (i.e., 1.5 to 1.7) except for some outliers at shallow/deep depths. Thus, it is suggested to use the reference value of 1.6 in normalized phase velocity to find the wavelength at Bukit Timah granite formation. Based on the apparent trend, the depth of bedrock is

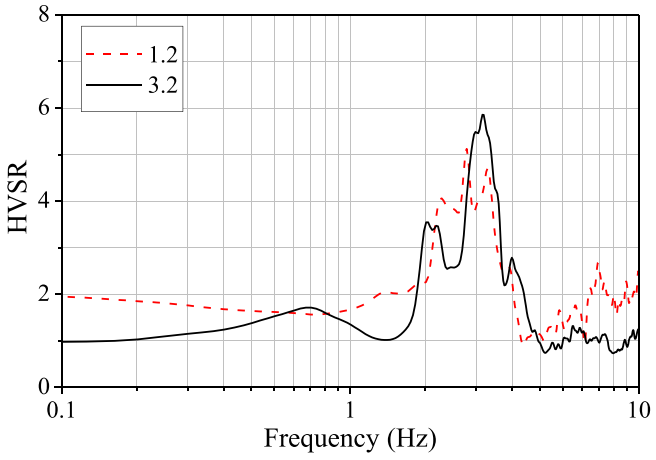

Fig. 8. HVSR at two borehole locations (#1.2 and #3.2).

Table 3
Comparison of the bedrock depths estimated using different approaches in this study.

Borehole #	Measured bedrock depth (m)	Estimated bedrock depth (m)					
		Bilinear Intersection	Pre-selected			Normalized V_R	H/V
			V_S	V_S-SD	V_S+SD		
1.1	34.3	41.0	34.8	30.2	39.6	38.3	31.2
1.2	39.9	37.0	34.8	30.2	34.8	39.3	35.9
2.1	25.8	27.0	27.8	24.2	N/A	27.7	25.1
2.2	25.5	23.0	36.4	23.7	N/A	25.7	27.5
3.1	31.0	31.0	27.5	24.1	N/A	29.3	29.1
3.2	28.5	32.0	31.6	27.8	N/A	35.3	30.8
4.1	10.0	11.0	10.0	8.0	N/A	9.0	8.4
4.2	13.9	25.0	24.2	20.8	27.8	13.3	14.9
5.1	45.5	47.0	44.6	34.8	60.7	36.7	43.5
5.2	41.2	42.0	39.6	30.2	60.7	38.3	45.0
6	24.4	27.0	23.7	20.9	28.0	24.7	26.1
7	31.0	30.0	36	26.8	N/A	N/A	36.9
8	18.5	20.0	24.2	20.8	31.6	26.0	21.8
9	32.0	32.1	N/A	35.7	N/A	32.1	31.8

Note: N/A: Not applicable, SD: Standard deviation.

recalculated to assess the prediction accuracy by adopting the reference value of 1.6, as shown in Table 3.

HVSR analyses are performed to estimate the natural frequencies of all test sites. The HVSR plots for all test sites are shown in Fig. 10. In this study, the effect of performance and sensitivity of 4.5 Hz geophones on HVSR would be ignored because main noise signals are generally measured around/above 4.5 Hz as shown in Fig. 11. In addition, the lower frequency geophone (e.g., 2 Hz) show only marginal improvement of accurate recordings compared to the 4.5 Hz geophone (Havskov, 2007; Strollo et al., 2008). The peaks are clearly determined for most of the plots, thus allowing the observation of natural frequencies of all test sites. The observed natural frequencies of all the tested sites are shown with the corresponding bedrock depths in Fig. 11. For Bukit Timah granite formation, a new empirical relationship between the natural frequency (f) and bedrock depth (D) is developed using a power function as follows:

$$D\,(m) = 92.5 \cdot f^{-1.06}(Hz), \quad R^2 = 0.94, \mathrm{RMSE} = 2.92 \tag{5}$$

where R^2 is a coefficient of determination and RMSE is a root-mean-square error. For comparison, two existing empirical correlation models developed by Ibs-von Seht and Wohlenberg (1999) and Parolai et al. (2002) are also shown together. It is found that two empirical relationship developed in previous studies underestimate the bedrock depth in Bukit Timah granite formation. In this study, the noted bedrock actually represents a weathered bedrock with grade III, which is different from

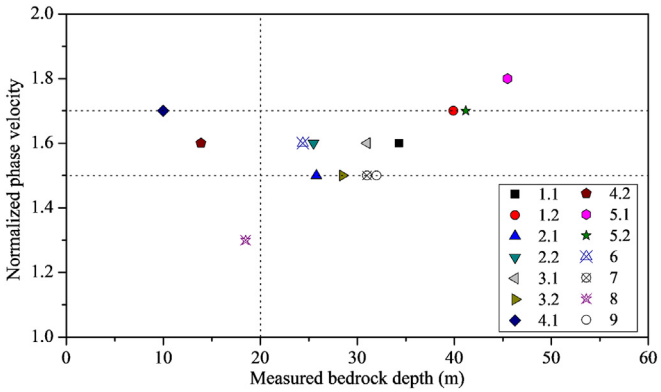

Fig. 9. Normalized phase velocity versus bedrock depth for all tested sites.

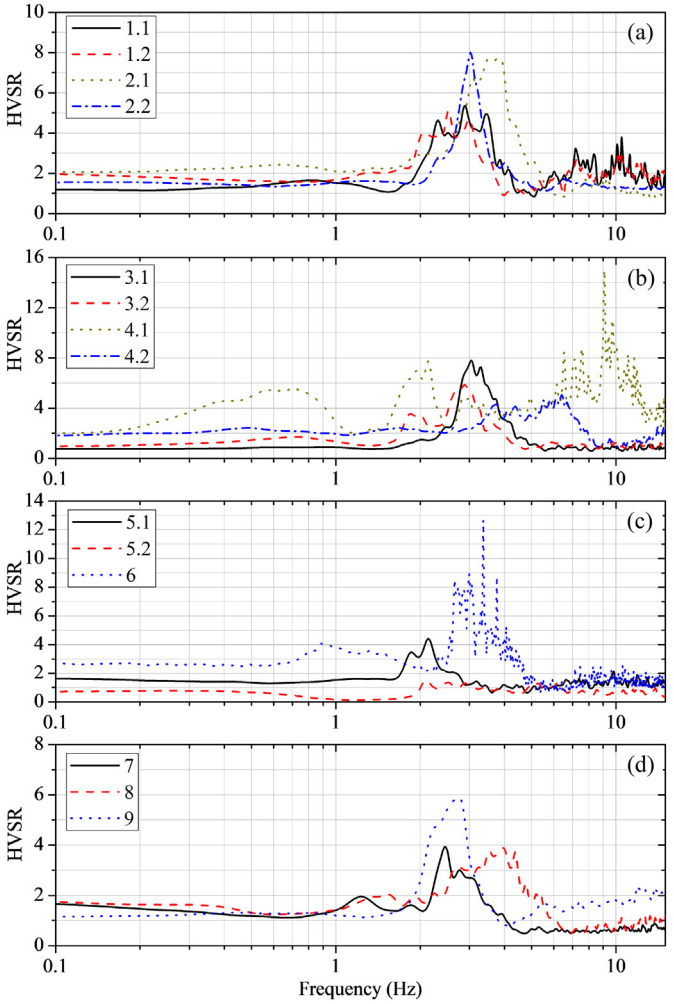

Fig. 10. HVSR for all tested sites: (a) #1.1, #1.2, #2.1, #2.2; (b) #3.1. #3.2, #4.1, #4.2; (c) #5.1, #5.2, #6; (d) #7, #8, #9.

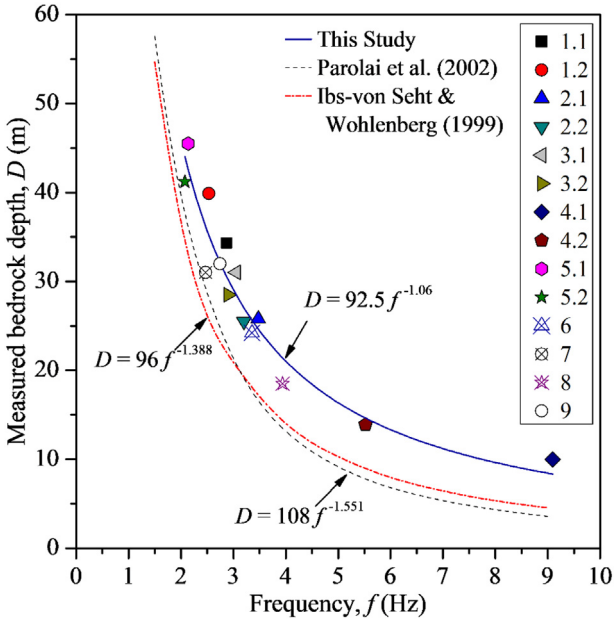

Fig. 11. Variation of bedrock depth with natural frequency at all test sites.

the intact rocks in previous studies. So, in this geologic condition, the V_S on bedrock surface is much lower and it may result in the disagreement with the previous empirical equations based on basement rocks. In addition, the depth dependency of V_S of the soil sediment would be relatively not significant due to the value of −1.06 in Eq. (5) which is closed to −1 ($f = V_S/\lambda$; $\lambda = 4D$). The depth of bedrock estimated from the Eq. (5) and the actual bedrock depth are listed in Table 3.

Fig. 12 compares the estimated bedrock depth to actual bedrock depth along with the line of equality, obtained from (1) bilinear intersection method, (2) preselected V_S-based approach, (3) normalized V_R-based approach, and (4) HVSR-based approach, respectively. From Fig. 12(a), it is seen that the bilinear intersection method gives reasonably good estimates ($R^2 = 0.87$; RMSE = 3.88) at most of the testing locations. The bilinear intersection method seems suitable for an initial estimation of the depth of bedrock. However, it would be only applicable in this site specific condition (e.g., weathered granite formation in Singapore). If the competent rock exists, it may not work due to the significant impedance contrast between upper soils and bedrock. From Fig. 12(b), it is understood that the preselected V_S-based approach is the least accurate method ($R^2 = 0.71$; RMSE = 5.59) among all the four proposed methods. However, the method can be still used as an initial estimate due to its easiness. It should be noted that the suggested average V_S of 456 m/s and/or average $V_S \pm$ SD are regional specific values which depend on the type of rock, degree of weathering and nature of rock formation. Therefore, the method should be used with caution and shall be employed with other suggested methods in this paper.

From the Fig. 12(c), it is observed that the normalized V_R based method predicts reasonably well ($R^2 = 0.84$; RMSE = 4.04) in most of the testing sites although the passive tests may result in poor estimates where bedrock is at shallow depth (< 20 m; i.e., at the shallow region where active-source surface wave is more appropriate). The considerable deviation shown in borehole #8 might be attributed to the lack of active-source data at such a shallow depth region. The selection of reference factor is important since it serves as a guide to predict the depth of bedrock.

Fig. 12(d) presents that the estimated bedrock depths using this HVSR are generally within 5 m deviation from the actual depths. It is indicated that the HVSR based approach gives relatively promising estimation of the depth of bedrock ($R^2 = 0.94$; RMSE = 2.92). It demonstrates that the new empirical relationship between the thickness of the overlying soil layer and natural frequency of the site can be successfully used to estimate the depth of bedrock at Bukit Timah granite formation. Moreover, the method uses only a single three-component geophone which is very easy to deploy without forming an array using multiple vertical component geophones. However, the empirical correlations are regional specific, and the accuracy of the proposed equation needs to be further tested for other regions.

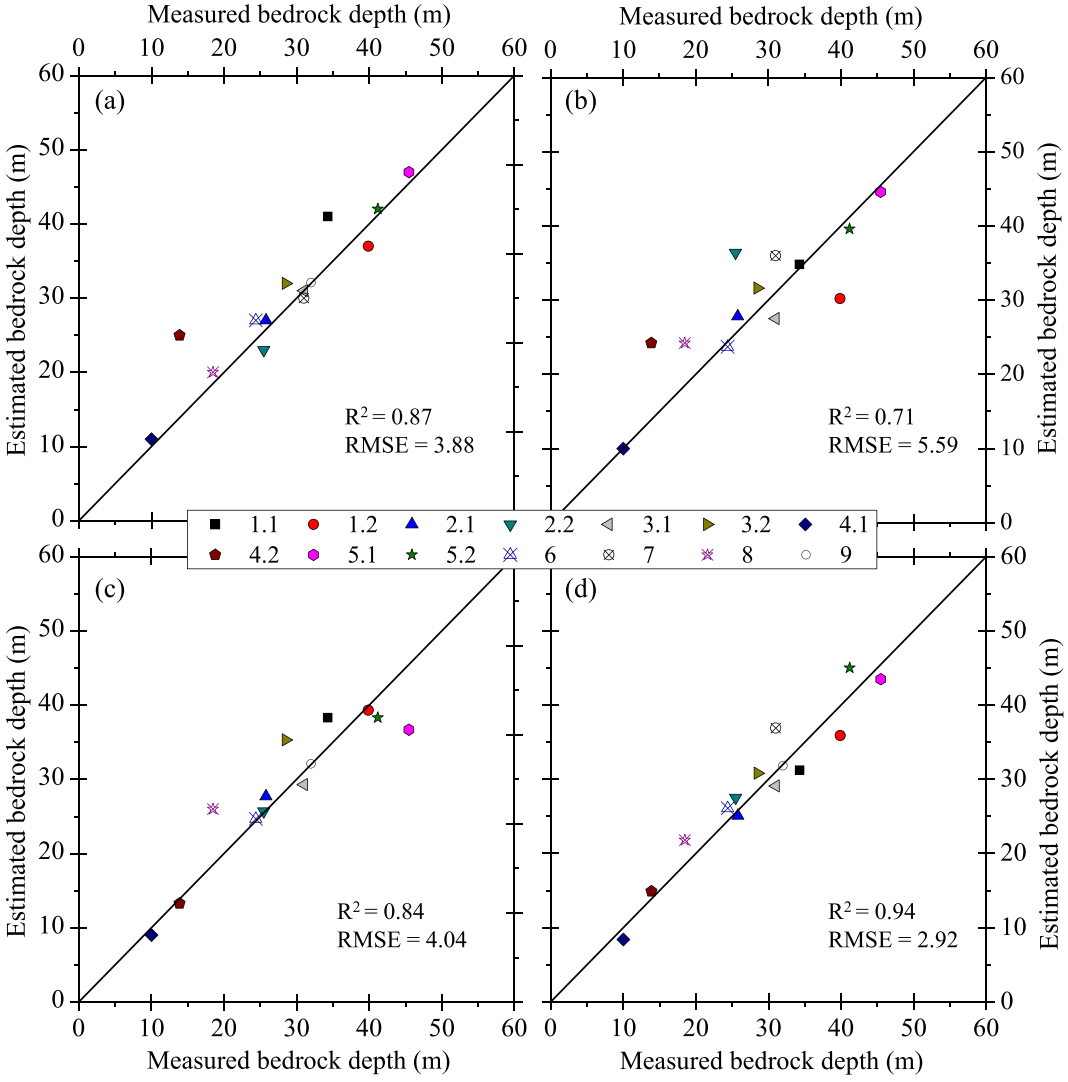

Fig. 12. Measured and estimated bedrock depth based on (a) bilinear intersection, (b) pre-selected V_s, (c) normalized V_R, and (d) HVSR.

6. Conclusions

Towards effective and eco-friendly detection of bedrock, a series of passive surface wave tests were performed at the Bukit Timah granite formation in Singapore. Four different approaches were proposed to estimate the depth of bedrock based on: 1) bilinear intersection; 2) preselected V_S; 3) normalized V_R; and 4) HVSR. Following key findings are made based on the experimental data analyses and test results.

- MAM test can be successfully used for bedrock detection, which is the low frequency ambient noise acquisition method. The method might be less confident at shallow depth based on SPAC method of signal processing. However, the method works well beyond the depth of 20 m. In such shallow cases, active MASW tests are recommended to be performed together to complete the V_S profile.
- Bilinear intersection and preselected V_S velocities may be used as an initial estimate. The bilinear intersection method is an intuitive graphical method which might be rather subjective. Since these two methods are based on the V_S profile (i.e., V_S vs. Depth) generated after an inversion process with a layered model by the SPAC method, non-uniqueness in the inversion process needs to be taken into account while using these two approaches. Thus, two approaches should be used together with the normalized V_R-based approach and/or the HVSR based approach.
- In the normalized V_R method, the recommended reference value to locate the wavelength for Bukit Timah granite formation region is 1.6. Although there are still outliers, the reference of 1.6 works generally well in this region. The approach can be applied similarly in other regions with calibration.
- The HVSR method employing MM seems to give better estimates of the depth of bedrock. In view of the simplicity of field acquisition, it is advisable to apply this approach for bedrock detection. As far as the V_S profile is also concerned, MAM is still required to carry out. It is also recommended to conduct both MAM and HVSR together to counter check each other.

Acknowledgement

The authors appreciate the financial support from Singapore Land Transport Authority (LTA, Award Number: R-302-000-164-490) and the Nazarbayev University (Grant No: 110119FD4508).

References

Aki, K., 1957. Space and time spectra of stationary stochastic waves, with special reference to microtremors. Bull. Earthq. Res. Ins. 35, 415–456.
Akkaya, İ., Özvan, A., 2019. Site characterization in the Van settlement (Eastern Turkey) using surface waves and HVSR microtremor methods. J. Appl. Geophys. 160, 157–170.
Anbazhagan, P., Sheikh, M.N., Parihar, A., 2012. Influence of rock depth on seismic site classification for shallow bedrock regions. Nat. Hazard. Rev. 14, 108–121.
Beauvais, A., Ritz, M., Parisot, J.-C., Dukhan, M., Bantsimba, C., 1999. Analysis of poorly stratified lateritic terrains overlying a granitic bedrock in West Africa, using 2-D electrical resistivity tomography. Earth Planet. Sci. Lett. 173, 413–424.
Coulouma, G., Tisseyre, B., Lagacherie, P., 2010. Is a Systematic Two-Dimensional EMI Soil Survey Always Relevant for Vineyard Production Management? A Test on Two Pedologically Contrasting Mediterranean Vineyards, Proximal Soil Sensing. Springer, pp. 283–295.
Del Gaudio, V., Wasowski, J., 2011. Advances and problems in understanding the seismic response of potentially unstable slopes. Eng. Geol. 122, 73–83.
Delgado, J., Casado, C.L., Estevez, A., Giner, J., Cuenca, A., Molina, S., 2000a. Mapping soft soils in the Segura river valley (SE Spain): a case study of microtremors as an exploration tool. J. Appl. Geophys. 45, 19–32.
Delgado, J., Casado, C.L., Giner, J., Estevez, A., Cuenca, A., Molina, S., 2000b. Microtremors as a geophysical exploration tool: applications and limitations. Pure Appl. Geophys. 157, 1445–1462.
Foti, S., Parolai, S., Albarello, D., Picozzi, M., 2011. Application of surface-wave methods for seismic site characterization. Surv. Geophys. 32, 777–825.
García-Jerez, A., Navarro, M., Alcalá, F., Luzón, F., Pérez-Ruiz, J., Enomoto, T., Vidal, F., Ocaña, E., 2007. Shallow velocity structure using joint inversion of array and h/v spectral ratio of ambient noise: the case of Mula town (SE of Spain). Soil Dyn. Earthq. Eng. 27, 907–919.
Havskov, J., 2007. Test of seismic recorders with 4.5 Hz sensors: GBV316 from GeoSig and SL07 from SARA. Norwegian National Seismic Network Technical Report.
Hayashi, K., 2008. Development of Surface-Wave Methods and its Application to Site Investigations. Kyoto University.
Ibs-von Seht, M., Wohlenberg, J., 1999. Microtremor measurements used to map thickness of soft sediments. Bull. Seismol. Soc. Am. 89, 250–259.
Institution, B.S., 1999. Code of practice for site investigations. BS 5930 1999.
Koesuma, S., Ridwan, M., Nugraha, A.D., Widiyantoro, S., Fukuda, Y., 2017. Preliminary estimation of engineering bedrock depths from microtremor array measurements in Solo, Central Java, Indonesia. J. Math. Fundam. Sci. 49, 306–320.
Kumar, B.S., Anbazhagan, P., Sitharam, T., 2006. Development of theoretical dispersion curves and comparison with multichannel analysis of surface waves (MASW). 13th Symposium on Earthquake Engineering. Indian Institute of Technology, Roorkee.
Lee, K.W., Zhou, Y., 2009. Geology of Singapore. Defence Science and Technology Agency, Singapore.
Lin, C.-P., Chang, C.-C., Chang, T.-S., 2004. The use of MASW method in the assessment of soil liquefaction potential. Soil Dyn. Earthq. Eng. 24, 689–698.
Malinowski, M., 2016. Deep reflection seismic imaging in SE Poland using extended correlation method applied to PolandSPAN™ data. Tectonophysics 689, 107–114.
Martínez, K., Mendoza, J.A., 2011. Urban seismic site investigations for a new metro in Central Copenhagen: near surface imaging using reflection, refraction and VSP methods. Phys. Chem. Earth Parts A/B/C 36, 1228–1236.
Moon, S.-W., Ku, T., 2017. Estimation of bedrock locations and weathering degree using shear wave velocity-based approach. Proceedings of the 19th International Conference on Soil Mechanics and Geotechnical Engineering (ICSMG), Seoul, South Korea.
Moon, S.-W., Ku, T., 2018. Undrained shear strength in cohesive soils estimated by directional modes of in-situ shear wave velocity. Geotech. Geol. Eng. 1–18.
Moon, S.-W., Khan, Q., Ku, T., 2016. Application of MASW methods for investigations of shear wave velocity in residual soils of Singapore. Geotech. Struct. Eng. Cong. 2016, 1688–1699.
Moon, S.-W., Hayashi, K., Ku, T., 2017. Estimating spatial variations in bedrock depth and weathering degree in decomposed granite from surface waves. J. Geotech. Geoenviron. Eng. 143, 04017020.
Moon, S.-W., Ng, Y.C., Ku, T., 2018. Global semi-empirical relationships for correlating soil unit weight with shear wave velocity by void-ratio function. Can. Geotech. J. 55, 1193–1197.
Nakamura, Y., 1989. A method for dynamic characteristics estimation of subsurface using microtremor on the ground surface Railway Technical Research Institute, Quarterly Reports 30.
Nazarian, S., Stokoe, K., 1984. In situ shear wave velocities from spectral analysis of surface waves. Proceedings of the World Conference on Earthquake Engineering. Prentice Hall San Francisco, California, pp. 21–28 July.
Okada, H., Suto, K., 2003. The Microtremor Survey Method. Society of Exploration Geophysicists with the cooperation of Society of Exploration Geophysicists of Japan [and] Australian Society of Exploration Geophysicists.
Parolai, S., Bormann, P., Milkereit, C., 2002. New relationships between Vs, thickness of sediments, and resonance frequency calculated by the H/V ratio of seismic noise for the Cologne area (Germany). Bull. Seismol. Soc. Am. 92, 2521–2527.
Pitts, J., 1983. The Origin, Nature and Extent of Recent Deposits in Singapore, Proceedings, 1st Int'l Seminar on Constructionproblems in Soft Soils. Nanyang Technological Institute, Singapore, pp. 1–18.
Rahardjoa, H., Aungb, K.K., Leongc, E.C., Rezaurd, R.B., 2004. Characteristics of residual soils in Singapore as formed by weathering. Eng. Geol. 73, 157–169.
Rezaei, S., Choobbasti, A.J., 2017. Application of the microtremor measurements to a site effect study. Earthq. Sci. 30, 157–164.
Rosenblad, B.L., Goetz, R., 2010. Study of the H/V spectral ratio method for determining average shear wave velocities in the Mississippi embayment. Eng. Geol. 112, 13–20.
Sharma, J., Chu, J., Zhao, J., 1999. Geological and geotechnical features of Singapore: an overview. Tunn. Undergr. Space Technol. 14, 419–431.
Sloan, S.D., Nolan, J.J., Broadfoot, S.W., McKenna, J.R., Metheny, O.M., 2013. Using near-surface seismic refraction tomography and multichannel analysis of surface waves to detect shallow tunnels: a feasibility study. J. Appl. Geophys. 99, 60–65.
Strollo, A., Bindi, D., Parolai, S., Jäckel, K.-H., 2008. On the suitability of 1 s geophone for ambient noise measurements in the 0.1–20Hz frequency range: experimental outcomes. Bull. Earthq. Eng. 6, 141–147.
Tamrakar, P., Luke, B., 2013. Feasibility of approximating depth to shallow bedrock directly from the Rayleigh wave dispersion curve. Geotech. Test. J. 36, 1–9.
Tokimatsu, K., Tamura, S., Kojima, H., 1992. Effects of multiple modes on Rayleigh wave dispersion characteristics. J. Geotech. Eng. 118, 1529–1543.
Winn, K., Rahardjo, H., Peng, S.C., 2001. Characterization of residual soils in Singapore. Geotech. Eng. 32, 1–13.
Xia, J., Miller, R.D., Park, C.B., 1999. Eastimation of near-surface shear wave velocity by inversion of Rayleigh waves. Geophysics 64, 691–700.
Zhang, Y., Ku, T., 2019. HVSR Measurement and Applications in Singapore, 16th Annual Meeting of Asia Oceania Geosciences Society (July 2019). Solid Earth Sciences – Geotechnical & Geophysical Site Characterization, Singapore, Session.
Zhao, J., 1998. Rock mass hydraulic conductivity of the Bukit Timah granite, Singapore. Eng. Geol. 50, 211–216.
Zhou, W., Beck, B., Stephenson, J., 2000. Reliability of dipole-dipole electrical resistivity tomography for defining depth to bedrock in covered karst terranes. Environ. Geol. 39, 760–766.